Power law rheology and strain-induced yielding in acidic solutions of type I-collagen

Frédéric Gobeaux,[a] Emmanuel Belamie,[b] Gervaise Mosser,[a] Patrick Davidson[c] and Sophie Asnacios*[de]

Received 22nd October 2009, Accepted 19th April 2010
DOI: 10.1039/b922151d

Acidic solutions of collagen are *in vitro* models of procollagen, the neutrosoluble precursor of collagen secreted by cells to build the extra-cellular matrix. Their viscoelastic properties may influence fibrils nucleation and growth during pH-triggered fibrillogenesis, and could thus be of particular interest for the engineering of artificial tissues as well as for the regulation of the structural properties of the extracellular matrix. Here we report on the rheological properties of acidic solutions of collagen over a wide concentration range, 0.6–300 mg mL^{-1}. At low concentrations, solutions display usual viscoelastic features consistent with those of dilute and semi-dilute solutions of macromolecules. At higher concentrations, both storage and loss moduli, G' and G'', scale as a weak power-law of the frequency ω^{α} ($\alpha = 0.15 - 0.3$), similar to what is reported for cross-linked actin networks, living cells and tissues. Creep experiments at high concentration reveal a weak power law regime at short times followed by a steady fluid-like regime at longer times. The transition between these two regimes appears at shorter times as stress amplitude increases. By rescaling creep responses, all time-domain data collapse onto a master curve. This defines a new time-stress superposition principle (TSS) and shows that fluidization occurs above a critical strain and after a lag-time scaling as $\sigma^{-1/\alpha}$. Power law rheology and strain-induced yielding are suggestive of soft-glassy rheology (SGR): concentrated collagen solutions would be close to a soft-glassy transition. Eventually, we compare the evolution of the rheological properties of acidic solutions from dilute to concentrated regimes to the non monotonous variation of fibrils diameter with collagen concentration in neutral gels.

Introduction

Some major connective tissues of vertebrates, such as bone, skin, cornea and tendon are mainly comprised of type I collagen, a 300 nm long protein formed by three polypeptide chains folded into a triple helix.[1] Collagen shows remarkable self-assembly properties at different length scales, from the formation of highly ordered cross-striated fibrils, to large, often periodic 3D networks supporting the extra-cellular matrix. The dimensions of the fibrils and their 3D organization appear to influence the mechanical and optical properties of biological or synthetic collagenous materials.[2] How structure is regulated to meet the functional requirements of different tissues remains an open question. Answering it would also have practical implications for the engineering of artificial tissues based on collagen matrices. Acidic solutions of collagen are usually considered as reasonable *in vitro* models of procollagen, the neutrosoluble precursor of collagen secreted by cells to build the extra-cellular matrix. Several key features of the *in vivo* 3D multiple scale architecture can be reproduced *in vitro* with acidic solutions of collagen, neutralized to yield strong fibrillar materials.[3–5] Although additional macromolecules co-secreted with procollagen have been shown to regulate the fibrils diameter, simple physicochemical parameters can therefore also influence the 3D assembly of collagen. Unexpectedly, the diameter of fibrils resulting from a pH increase in acidic solutions of collagen varies non-monotonously across a wide range of collagen concentration.[4–9] To assess whether fibril nucleation and growth processes could be influenced by the viscoelastic properties of the initial collagen solutions, we have characterized the rheological properties of acidic collagen solutions over a wide concentration range.

From a physico-chemical point of view, type I collagen in solution is usually considered as a charged semiflexible macromolecule (with the contour length $L = 300$ nm and a persistence length L_P in the range 57–160 nm[10–13]). Although mechanical properties of flexible and rod-like polymers have been described since the late 1970s,[14] the distinctive features of semiflexible polymers have only recently begun to be explored both experimentally and theoretically.[15,16] Most studies on semiflexibility were carried on F-actin, one of the major cytoskeletal elements involved in cell mechanics. Besides semiflexibility, the influence of enthalpic interactions between chains on the mechanical properties of polymer solutions and networks also remains of current interest.

With a few exceptions,[17] previous rheological studies on collagen have primarily focused either on the formation of fibrils from dilute solutions and the resulting sol–gel transition, pH- or heat-triggered,[18,19] or on fibrillar gels.[20,21] In this work, we have

[a]*Laboratoire de Chimie de la Matière Condensée de Paris, UMR 7574 CNRS, Université Pierre et Marie Curie, France*
[b]*Laboratoire "Matériaux du Vivant et Vectorisation" de l'Ecole Pratique des Hautes Etudes, Institut Charles Gerhardt, UMR 5253 CNRS, Ecole de Chimie Montpellier/UM2/UM1, 8 rue de l'Ecole Normale, 34296 Montpellier Cedex 5, France*
[c]*Laboratoire de Physique des Solides, UMR 8502 CNRS, Université Paris Sud, Bât. 510, 91405 Orsay Cedex, France*
[d]*Laboratoire Matière et Systèmes Complexes (MSC), UMR 7057 CNRS & Université Paris Diderot, 10 rue Alice Domon et Léonie Duquet, 75205 Paris Cédex 13, France. E-mail: sophie.asnacios@univ-paris-diderot.fr*
[e]*UPMC Univ Paris 06, Dept Phys, F-75005 Paris, France*

investigated the mechanical properties of solutions of type I collagen molecules, at acidic pH (500 mM acetic acid) over a wide concentration range (0.6–300 mg mL^{-1}) by means of rotating disk rheometry, without inducing fibrillogenesis.

We first present low amplitude oscillatory experiments and steady shear tests. At low concentrations, solutions display viscoelastic features consistent with dilute and semi-dilute regimes. Steady shear experiments enabled to determine the overlap concentration c^* separating dilute from semi-dilute regimes. At higher concentrations, both storage and loss modulus exhibit power law behaviours ($G',G'' \propto \omega^{\alpha}$) with $\alpha \approx 0.3$ in the (27–112 mg mL^{-1}) range and $\alpha \approx 0.15$ for $C = 300$ mg mL^{-1}. We then compare these data to a previous SAXS investigation[22] on similar solutions.

The second part of the result section is devoted to creep measurements performed for one single concentration (27 mg mL^{-1}) in the concentrated regime. Using an original time-stress superposition principle (TSS), we show that the strain-*versus*-time curves $\gamma(t)$ obtained for various stress amplitudes σ, all rescale onto a master curve. This master curve reveals a power law regime at short times in which $\gamma(t) \propto \sigma t^{\alpha}$, followed by a steady-state fluid-like regime in which $\gamma(t) \propto \sigma^{1/\alpha} t$. The fluidization occurs after a lag time scaling as $\sigma^{-1/\alpha}$.

These results are then discussed in the framework of models assuming either partial gelation,[23] hierarchical structure[24] or disorder and metastability in the solutions (soft glassy rheology, SGR model[25]). In the last part of the discussion, we compare the rheological properties of the acidic solutions from dilute to concentrated regimes to the non monotonous evolution of fibrils diameter with collagen concentration obtained in the corresponding neutral gels.

Materials and methods

Collagen extraction and purification

Type I collagen was extracted from the tail tendons of young Wistar rats.[5] The tendons were excised in a sterile flow hood and washed with phosphate-buffered saline (PBS, 137 mM NaCl, 2.68 mM KCl, 8.07 mM Na_2HPO_4, and 1.47 mM NaH_2PO_4) to remove cells and traces of blood. The tissues were then soaked in a 4 M NaCl solution to lyse remaining cells and precipitate some of the high-molecular-weight proteins. The tendons were then rinsed again with PBS and solubilized in 500 mM acetic acid. The solution was clarified by centrifugation at 41 000 × *g* for 2 h. Proteins other than type I collagen were selectively precipitated in 300 mM NaCl and removed by centrifugation at 41 000 × *g* for 3 h. Collagen was retrieved from the supernatant by precipitation in 600 mM NaCl and centrifugation at 3000 × *g* for 45 min. The pellets were solubilized in 500 mM acetic acid and thoroughly dialysed against the same solvent to completely remove NaCl. The solutions were kept at 4 °C and centrifuged at 41 000 × *g* for 4 h before use. Sample purity was assessed by SDS-PAGE electrophoresis. Given the quantities necessary for our experiments, very stringent purification was not possible and traces of other components may remain.

Concentration and titration

A stock solution at approximately 5 mg ml^{-1} was concentrated to the desired concentration by reverse dialysis against polyethylene glycol (35 kDa, Fluka) dissolved in 500 mM acetic acid, (corresponding to a pH of 2.5) up to 30% (w/v). Final collagen concentration was determined by assessing the amount of hydroxyproline.[26] Concentrations below 5 mg ml^{-1} were obtained through successive dilutions in 500 mM acetic acid. The air bubbles trapped in the most concentrated solutions were removed by centrifugation at 3000 × *g* for a few minutes to ensure the homogeneity of the measurements.

Rheological measurements

Rheological measurements were carried on in a cone-and-plate cell (40 mm in diameter, angle of 0.04 rad, SR500 Rheometrics). The temperature was controlled using water circulating from a thermo regulated bath. The rheological tests were performed at $T = 20 \pm 0.1$ °C. The top of the cell was covered with a lid and the atmosphere inside the cell was saturated with a 500 mM acetic solution to minimize solvent evaporation.

We performed steady shear tests to determine the overlap concentration, low amplitude oscillatory tests and creep experiments to measure linear and non linear responses respectively. Before each oscillatory experiment, the sample was brought to the same initial state by a controlled history of shear and rest: it was first sheared during 300 s at a constant shear rate (8 s^{-1}) then left at rest for one hour before starting small-amplitude oscillatory experiments. We explicitly checked for the extent of the linear regime by performing amplitude sweeps at 1 rad s^{-1}: upper-limits of the linear regime were found between 50 and 100%. The storage and loss modulus (respectively G' and G'') were measured by applying a frequency sweep over three decades (0.01–30 rad s^{-1}), with a strain amplitude of 10%, on the same sample. In creep experiments, a constant stress was applied to the sample and the compliance $J(t)$, defined as the ratio between the resulting strain and the applied stress (γ/σ), was measured as a function of time. Creep experiments at different stress amplitudes (20–150 Pa) were performed for a single concentration (27 mg ml^{-1}). Recovery data measured after each creep test show that the relaxation time is about an hour (this point is documented below).

Results

Dilute, semi-dilute and concentrated regimes

Rheological measurements. At low concentration ($c \leq$ 16 mg mL^{-1}), steady shear experiments enabled to determine the upper limit of the dilute regime. Reduced viscosity values η_{sp}/c were determined from viscosities dependence on shear rate (Newtonian plateau values, Fig. 1). η_{sp}/c was then plotted as a function of collagen concentration (Fig. 2). Extrapolating η_{sp}/c at zero concentration, we found an intrinsic viscosity value $[\eta] = 765 \pm 110$ mL g^{-1}. This result is rather close to the value reported[28] previously ($[\eta] = 865$ mL g^{-1} for Mw = 300 kDa) for similar solutions of collagen at pH = 3.7 (against pH = 2.5 in our case).

The overlap concentration c^* separating the dilute from semidilute regime was then estimated from the intrinsic viscosity $[\eta]$. Indeed, theoretical predictions[27] based on space-filling considerations lead to $0.7 < c^*[\eta] < 1.5$. We thus found 1 mg $mL^{-1} < c^* < 2.5$ mg mL^{-1}.

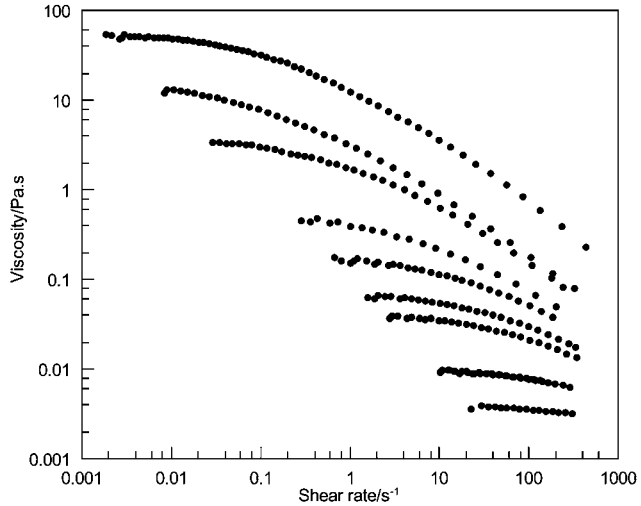

Fig. 1 Steady viscosity η against strain rate $\dot{\gamma}$ for various collagen concentrations 0.6mg mL^{-1} $\leq c \leq$ 16 mg mL^{-1}.

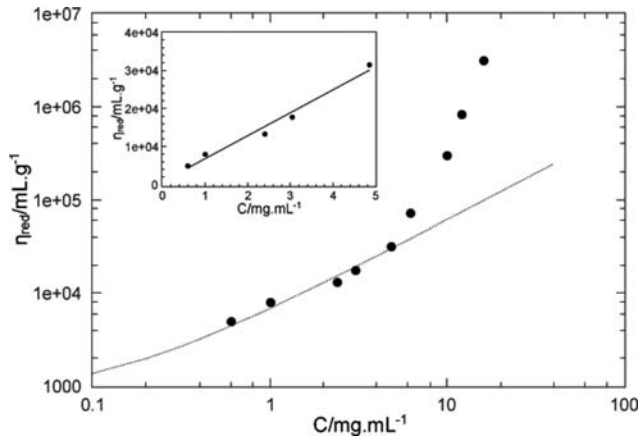

Fig. 2 Reduced viscosity η_{sp}/c against collagen concentration c (log/log plot). Dashed line: linear fit. Insert: Reduced viscosity η_{sp}/C against collagen concentration c (lin/lin plot). Linear fit (solid line) gives $\lim_{C\to 0} \eta_{sp}/c = [\eta] = 765 \pm 110$ mL/g.

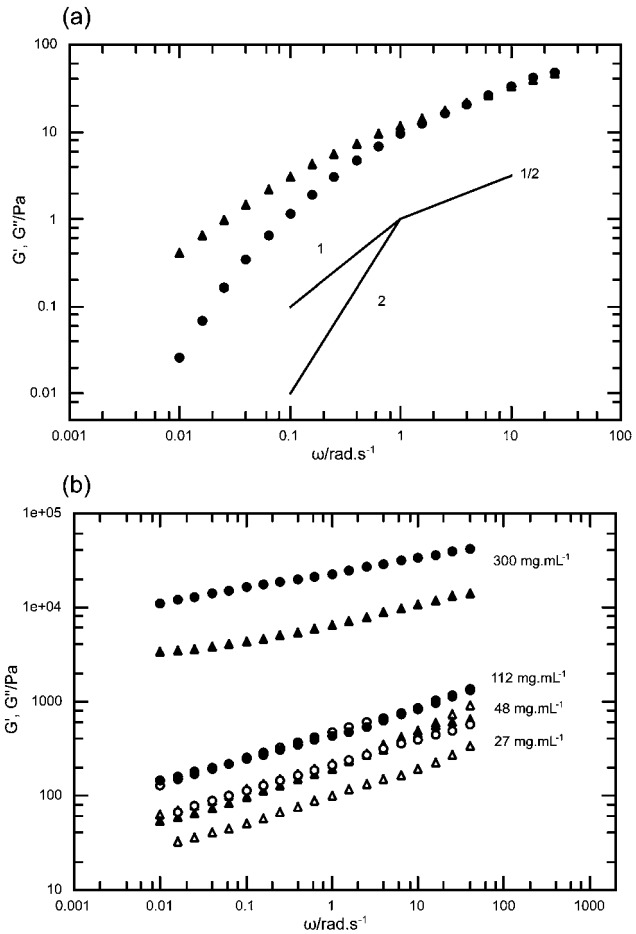

Fig. 3 Shear storage G' (O) and loss G'' ($\triangle$) moduli against frequency (a) at 16 mg mL^{-1}; (b) at 27 mg mL^{-1}, 48 mg mL^{-1}, 112 mg mL^{-1}, and 300 mg mL^{-1}. The frequency dependence of G' and G'' is well described by power laws: $G'(\omega) = G_0'\left(\frac{\omega}{\omega_0}\right)^{\beta}$ and $G''(\omega) = G_0''\left(\frac{\omega}{\omega_0}\right)^{\beta}$ with $\omega_0 = 1$ rad s^{-1}, $\beta = 0.3 \pm 0.02$ for 27 to 112 mg mL^{-1} and $\beta = 0.15$ for 300 mg mL^{-1}.

It is noteworthy that determining c^* from the departure of the η_{sp}/c curve from the slope 1 (Huggins' equation), leads to 3 mg mL^{-1} < c^* < 5mg mL^{-1} with $c^* \sim 1/[\eta]$.

We then focus on the rheological properties of collagen solutions at higher concentrations ($c \geq 16$ mg mL^{-1}). Oscillatory experiments showed a trend from ordinary viscoelastic behaviour of semidilute solutions at 16 mg mL^{-1} to power law viscoelastic spectra for higher concentrations.

At 16 mg ml^{-1} (Fig. 3a) G' and G'' respectively scale as ω^2 and ω in the low frequency limit. This is consistent with the predicted terminal maxwellian behaviour[29] resulting from one dominant molecular relaxation process. In the high frequency limit, G' approaches G'', both scaling as $\omega^{1/2}$. This frequency dependence is usually observed for macromolecules in semidilute regimes when overlapping between coils cancels the hydrodynamic interactions between different portions of the same molecule.[14]

For concentrations higher than 27 mg mL^{-1} (Fig. 3b), solutions exhibit a rather different behaviour with a power-law frequency dependence of both moduli over three orders of magnitude, and $G'(\omega) = G_0'\left(\frac{\omega}{\omega_0}\right)^{\beta} > G''(\omega) = G_0''\left(\frac{\omega}{\omega_0}\right)^{\beta}$, with $\omega_0 = 1$ rad s^{-1} (Fig. 2). This behaviour differs from the ordinary viscoelastic properties of concentrated solutions of macromolecules whose viscoelasticity is usually dominated by steric entanglements leading to distinct behaviours of storage and loss moduli (respectively plateau and non-monotonous frequency dependence). The power-law behaviour is conserved over a wide collagen concentration range as indicated by nearly constant values of the exponent $\beta = 0.3 \pm 0.02$ and prefactors $G_0' = 460 \pm 20$ Pa and $G_0'' = 230 \pm 30$ Pa (Fig. 4). Only the most concentrated sample (300 mg mL^{-1}) displays a lower value of β ($\beta = 0.15$) and prefactors two orders of magnitude higher ($G_0' \approx 23\,200$ Pa and $G_0'' \approx 6200$ Pa) than in the 27–112 mg mL^{-1} range.

Comparison to previous SAXS investigation. In this section, we consider the rheological data reported above in the light of a previous SAXS (small angle X-ray scattering) investigation performed on similar collagen solutions.[22] In the dilute and

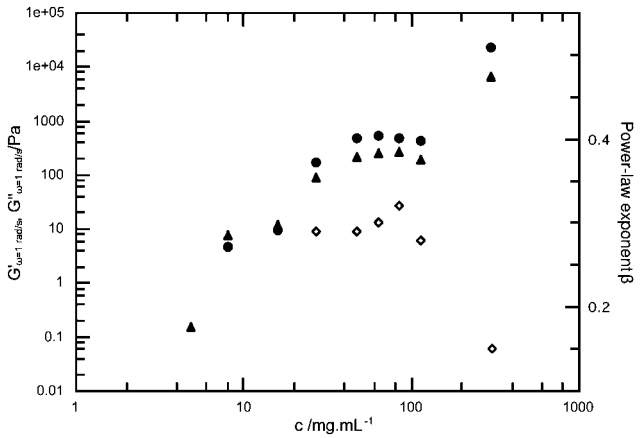

Fig. 4 Prefactors $G'(\omega_0 = 1 \text{ rad s}^{-1}) = G'_0$ (○), $G''(\omega_0 = 1 \text{ rad s}^{-1}) = G''_0$ (△) and power-law exponent β against collagen concentration c.

semi-dilute regimes ($c \leq 16$ mg mL^{-1}), SAXS patterns were weak and isotropic with no detectable local order.

Beyond about 20 mg mL^{-1}, the presence of a broad SAXS interference peak revealed a liquid-like positional order. The average distance between triple helices inferred from the peak position varied as $\phi^{-1/2}$ (with ϕ the collagen volume fraction) indicating that the molecules' axes were set on a 2D lattice. SAXS investigations also revealed that the interference peak, indicative of predominantly repulsive interactions, increased and broadened as collagen concentration increased, until it vanished for concentrations beyond 166 mg mL^{-1}. Dominant repulsive interactions arise from the excess of positive charges (277) of collagen molecules at pH = 2.5. Repulsive interactions together with a strong susceptibility to shear suggested a tendency to local orientational order[30–33] in isotropic solutions. An isotropic-to-nematic transition occurs at about 60 mg mL^{-1}. Equilibrium concentrations and the order parameter of the nematic phase agreed reasonably well with theoretical predictions for semi-flexible macromolecules with Lp estimated between 50 and 110 nm. It is noteworthy that in almost the same concentration range of dominantly repulsive interactions (27–112 mg mL^{-1}), suspensions exhibit power law spectra with fairly constant parameters ($\beta \sim 0.3$, G'_0 and G''_0) (Fig. 3).

Beyond 166 mg mL^{-1}, SAXS showed that repulsions, dominant at lower volume fraction, were overcome by attractive interactions at high packing densities. Native-like fibrils even formed spontaneously in the acidic solutions,[5] consequently to the self-assembly of triple helices induced by short-range attractive interactions. The highest concentration (c = 300 mg mL^{-1}) investigated by rheometry lies well beyond this limit evidenced by SAXS (c > 166 mg mL^{-1}). This suggests that the transition from repulsive to attractive regimes evidenced by SAXS seems to be related to the change in the value of β, G'_0 and G''_0.

Yielding in creep experiments

In the following, we present shear compliance data, obtained at one collagen concentration (27 mg mL^{-1}). This concentration was representative of the samples in the 27 to 112 mg mL^{-1} range, for which the power-law exponent β in oscillatory experiments was found to be constant ($\beta = 0.3$).

Time-stress superposition principle. Successive creep-recovery runs were carried on from 20 to 150 Pa. Preliminary tests had indicated: (i) that creep curves were not reproducible when the sample had not completely relaxed from the previous creep run (ii) that the relaxation was all the more fast than the amplitude of the applied stress in the creep period was high. As the relaxation time for 20 Pa was about 2500 s, we thus chose a recovery period of 2500 s for each run. Compliance curves, $J(t,\sigma) = \frac{\gamma(t)}{\sigma}$, obtained for the individual runs from 20 to 150 Pa are reported in Fig. 5. Corresponding recovery data are presented in Fig. 6.

For the lower stress values, $J(t)$ is a weak power-law of the time: $J(t) \sim t^{\alpha}(\alpha = 0.29)$. Under moderate stress, $J(t)$ exhibits two successive regimes over time: J scales as t^{α} with $\alpha = 0.29$ at short times and with $\alpha = 1$ at longer times. The higher the stress applied, the sooner the slope change occurs. This suggests that the individual curves $J(t,\sigma)$ could essentially result from the same response function, shifted along the time and compliance axes, according to the value of the applied stress. All experimental curves indeed collapse onto a master curve $J_R(t/a_\sigma)$ (Fig. 7) when a rescaling procedure is applied to our data (see Appendix for details). Reduced compliance J_R actually corresponds to the strain γ, and the time shifting factor a_σ varies with stress as $\sigma^{-1/\alpha}$. This "time–stress superposition principle" implies that an increase in the applied stress accelerates similarly all the relaxation processes. The relaxation spectrum is therefore shifted towards the region of shorter times without changing its shape: characteristic times all scale as $\sigma^{-1/\alpha}$.

The master curve $\gamma(t/a_\sigma)$ thus reveals that for any applied stress the solution exhibits two successive regimes of strain: a short time regime in which strain scales as $(t/a_\sigma)^{\alpha}$, followed by a long time regime in which strain scales as (t/a_σ). Note that the terms "short time" and "long time" refer to the normalized time (t/a_σ).

Linear regime and dominant solid-like behaviour at short-time. The short-time regime corresponds to the linear deformation

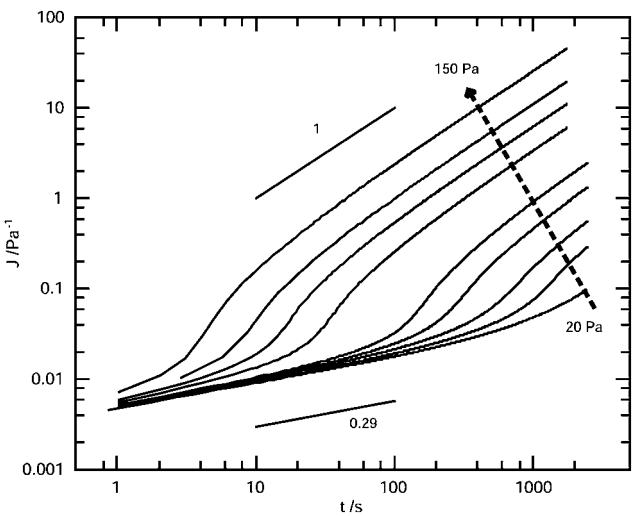

Fig. 5 Creep compliance $J(t) = \frac{\gamma(t)}{\sigma}$ against time for σ = 20, 25, 30, 40, 50, 80, 100, 120, 150 Pa for c = 27 mg mL^{-1}. At short times, $J(t) = At^{\alpha}$ (with $A = 4.9.10^{-3}$ Pa^{-1} s$^{-\alpha}$ and $\alpha = 0.29$) whereas $J(t) \sim t$ at long times.

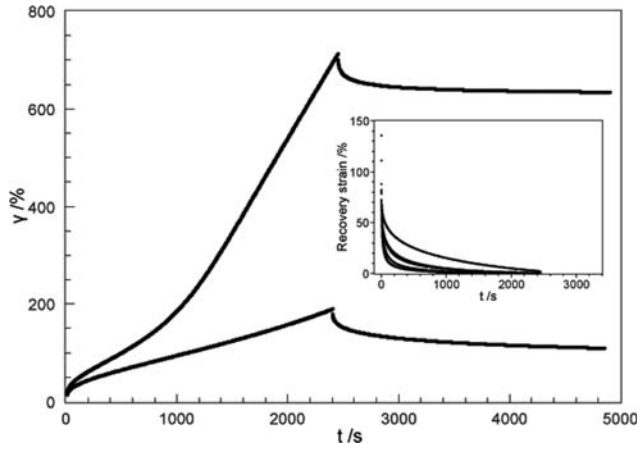

Fig. 6 Creep-recovery data: strain γ against time t for $\sigma = 20$, 25 Pa. Insert: Recovery curves from $\sigma = 20$, 25, 30, 40, 50 Pa. Normalized recovery data $\gamma(t) - \gamma_\infty$ are plotted against elapsed time from stress arrest. The longest relaxation time about 2500 s corresponds to recovery from the lowest stress $\sigma = 20$ Pa.

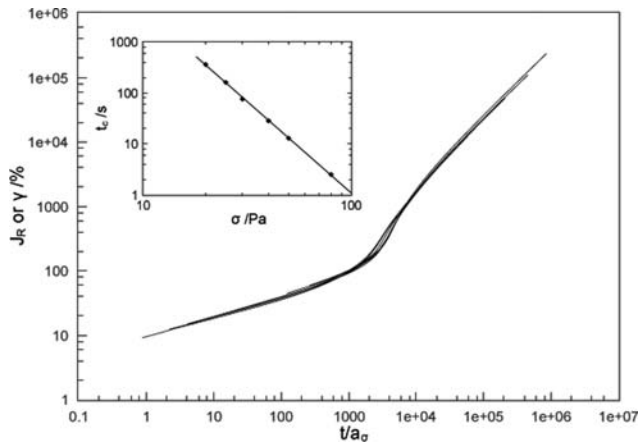

Fig. 7 Reduced creep compliance J_R or strain γ against reduced time. $\frac{t}{a_\sigma}$, for $\sigma = 20$, 25, 30, 40, 50, 80, 100, 120, 150 Pa. Data are shifted in time to the arbitrary chosen reference curve ($\sigma_0 = 20$ Pa) for which one has $a_\sigma(\sigma_0) = 1$ (see appendix). Curves collapse onto a master-curve displaying strain-induced yielding from $J_R \sim \left(\frac{t}{a_\sigma}\right)^\alpha$ to $J_R \sim \left(\frac{t}{a_\sigma}\right)$. It occurs beyond a critical strain γ_C of about 50%. Insert: Lag time before fluidization t_C against stress σ, well fitted by $t_C \approx 1.59.10^7\sigma^{-3.58}$ (*solid line*) in agreement with $t_C = \left(\frac{50\%}{A\sigma}\right)^{1/\alpha}$ (with $A = 4.9.10^{-3}$ Pa^{-1} s$^{-\alpha}$ and $\alpha = 0.29$ from Fig. 5).

regime since it is characterized by a linear relationship between strain and stress: $\gamma(t) = (At^\alpha)\sigma$ where $A = 4.9.10^{-3}$ s$^{-\alpha}$ Pa^{-1} s and $\alpha = 0.29$, regardless of the value of the applied stress. Indeed, compliances obtained at different applied stress values have quantitatively the same time evolution at short time (Fig. 4). The theory of linear viscoelasticity predicts equivalence between creep and oscillatory measurements provided there is a linear relationship between stress and strain: the features of time-response correspond to those of frequency-response through Laplace transformations.[34] Thus, if the complex modulus ($G^*(\omega) = G'(\omega) + iG''(\omega)$) is a weak power-law of the frequency, the creep function is a weak power-law of the time with the same exponent and $G^* = \frac{(i\omega)^\alpha}{A\Gamma(1+\alpha)}$, with $\Gamma(x)$ the gamma function.[34] Experimentally, we found that $\alpha \approx \beta \approx 0.3$ and the value of G_0' calculated from A and α ($G_0' = \frac{\cos(\alpha\pi/2)}{A\Gamma(1+\alpha)}\omega^\alpha = 221 \pm 9Pa$) is in good agreement with those from oscillatory tests, reported in Fig. 3 ($G_0' = 207 \pm 14$ Pa). In the following, the "power law behaviour" will refer indifferently to the time dependence of J, or to the frequency dependence of G^*.

The value of the exponent α (or β) reflects a dominantly solid-like or liquid-like behaviour of the sample.[29] Indeed, according to their definitions and in the case of a power law behaviour, the storage (G') and loss (G'') moduli are characterized by the following relation: $\tan\left(\alpha\frac{\pi}{2}\right) = \frac{G''}{G'}$. The two characteristic limits are $\alpha(=\beta) = 0$ for a Hookean solid, characterized by a purely elastic deformation with no dissipation ($G''(\omega) = 0$) and $\alpha(=\beta) = 1$ for a viscous fluid ($G'(\omega) = 0$). Concentrated solutions thus exhibit a dominant solid-like behaviour ($\alpha = 0.29 < 0.5$) in the linear regime (*i.e.* in oscillatory experiments and in creep experiments at short times).

Strain-induced yielding. At long times the 27 mg mL^{-1} collagen solution flows as a fluid. According to TSS, the relationship between strain and stress is no more linear, with $\gamma \sim \frac{t}{a_\sigma} = t\sigma^{1/\alpha}$. This time dependence of the strain corresponds to a shear-thinning steady-state flow. Indeed, it follows from $\gamma \sim t\sigma^{1/\alpha}$ that the strain rate $\dot{\gamma}(t) = \frac{d\gamma}{dt}$ is constant in time ($\dot{\gamma}_{SS}$), and is proportional to $\sigma^{1/\alpha}$. The apparent viscosity should thus decrease as $\dot{\gamma}^{\alpha-1}$with increasing strain rate. The flow curve (Fig. 8) obtained by plotting the applied stress as a function of the final shear rate in the creep tests is well fitted by $\sigma = C\dot{\gamma}_{ss}^n$ with $n = 0.27$. This value is very close to the value of α (0.29) characterizing the transient short-time regime. This is consistent with TSS principle: the

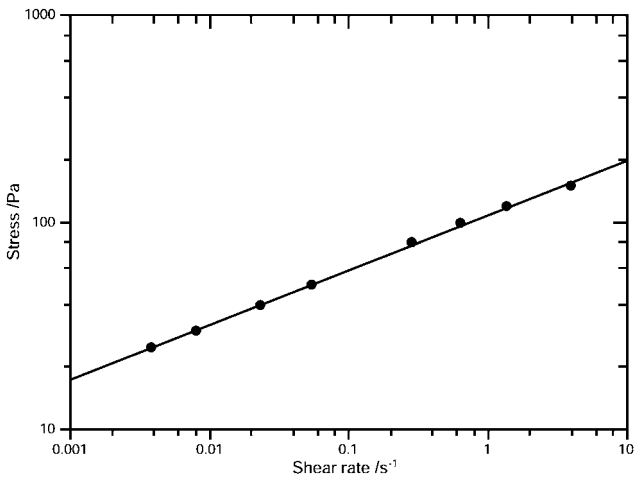

Fig. 8 Flow curve for $c = 27$ mg mL^{-1}. Stress σ against steady shear rate $\dot{\gamma}$ from creep tests, well fitted by $\sigma = K\dot{\gamma}^n$ with $n \approx 0.27$ which is very close to $\alpha = 0.29$ characterizing the transient short-time regime in the creep tests.

exponent of the creep function in the transient linear regime ($J(t) = At^{\alpha}$) and the exponent characterizing the steady-state shear-thinning regime ($\sigma \sim \dot{\gamma}_{ss}^{\alpha}$) are expected to be the same.

The master curve $\gamma(t/a_{\sigma})$ thus shows that concentrated solutions submitted to a constant stress exhibit yielding from a linear regime of deformation dominated by elastic storage to a nonlinear steady-state dissipative flow.

This yielding is strain-induced. Indeed, regardless of the applied stress, yielding starts when the total deformation of the solution reaches a critical value γ_C, about 50%. This result is in good agreement with the amplitude sweep in oscillatory experiments. The elapsed time t_C to reach γ_C can be deduced from $t_C/a_{\sigma} = \left(\frac{\gamma_C}{A\sigma_0}\right)^{1/\alpha}$ according to eqn (4) of the appendix. t_C is thus stress dependent : $t_C = \left(\frac{\gamma_C}{A\sigma}\right)^{1/\alpha}$. It spans from 1 s at $\sigma = 150$ Pa, to a few minutes at $\sigma = 20$ Pa, as shown in Fig. 7 (insert). Moreover, the lag time to reach the steady-state for a given stress σ can be deduced from the value of such a lag time for one reference stress: $t_{SS}(\sigma) = \left(\frac{\sigma_{ref}}{\sigma}\right)^{1/\alpha} t_{SS}(\sigma_{ref})$. Taking one minute for 80 Pa (Fig. 5), we obtain that $t_{SS}(\sigma)$ spans from a few seconds at $\sigma = 150$ Pa to two hours at $\sigma = 20$ Pa.

For 300 mg mL^{-1}, strain-induced yielding could not be reached within accessible time scales nor within accessible stress scales. We thus could not assess the consistency of TSS for more solid-like conditions ($\alpha = 0.15$).

Discussion

Power-law rheology, strain-induced yielding and TSS

A previous study[17] reported that viscoelastic moduli of a 1.5% collagen solution (500 mM acetic acid) scaled respectively as $G' \sim \omega^{0.26}$ and $G'' \sim \omega^{0.19}$. Except a small shift in concentration and in exponent values, this is rather close to our results: we found that G' and G'' scaled as $\omega^{0.3}$ for $C \geq 27$ mg mL^{-1} (about 2.7%). Nevertheless, the exponents for G' and G'' differed and the authors analyzed this result in the framework of the three-zone-model which is the current model[14,29] to analyze the viscoelastic properties of solutions of macromolecules with dominant steric interactions. $G' \sim \omega^{0.26}$ and $G'' \sim \omega^{0.19}$ behaviours were interpreted as the plateau zone resulting from topological entanglements that lock the solution structure into a temporary network with a fixed elastic moduli. Viscoelastic properties of a three-zone kind are characterized by a discrete number of distinct relaxation time scales. In contrast, our data at 27 mg mL^{-1} clearly show power-law behavior with the same exponent for G′ and G″. Moreover, SAXS data revealed dominant repulsive interactions and a tendency to local orientational order which are unfavourable to entanglements between macromolecules. Unlike plateau zone, power law spectra correspond to a broad and dense distribution of relaxation times: no particular internal time dominates. Power law rheology also indicate that elastic and dissipative properties share a common underlying mechanism, since the ratio of both modulus $G'(\omega) \Big/ G''(\omega)$ is frequency free.

During the last decades, weak power-law viscoelasticity has been reported for soft materials (critical gels, dense emulsions, foams) as well as for living cells,[34–36] tissues,[37] *in vitro* cytoskeletal cross-linked networks.[38] Two models describing power-law viscoelasticity have been proposed.

The first theoretical approach considers that the large and broad distribution of relaxation times originates from the formation of a hierarchical structure, where a characteristic mechanical pattern is reproduced at different spatial scales. This is found, for example, at the gel point for the partially gelled liquids formed on the way toward complete gelation[23] or in multiple-scale cellular actin networks comprised of individual actin filaments, bundles and stress fibers.[24] In the concentration range 27–112 mg mL^{-1} where both moduli scaled as $\omega^{0.3}$, our data do not really support the hypothesis of such a growing hierarchical structure. Actually SAXS experiments[22] clearly indicated that repulsive interactions between triple helices dominated, limiting the formation of an interconnected structure or aggregates of significantly different sizes. Nevertheless, for the most concentrated sample (300 mg mL^{-1}), the assumption of a hierarchical structure is however possible, since attractive interactions dominate and since fibrils were observed to spontaneously form (without any pH change).

Another model, called the "soft glassy rheology" (SGR) considers that the systems mechanics is controlled by disorder, metastability and local structural rearrangements.[25] Thermal motion alone is not sufficient to achieve complete structural relaxation. Mechanical energy associated to local rearrangements between mesoscopic elements can nevertheless help the system to cross multiple high energy barriers. The system can be driven into a glassy, liquid, or intermediate state through a mechanically-activated process characterized by a mean-field "noise temperature", x.

For the intermediate state, near but above the (soft) glass transition, ($1 < x < 2$), SGR predicts that both storage and loss moduli are a weak power-law of shear frequency, with the same exponent: $x - 1$. The experimental power exponent we found in the 27–112 mg mL^{-1} range thus suggests fitting to the SGR model at $x = 1.3$: concentrated collagen solutions would be in a "nearby glassy state" between the glass ($x < 1$) and the liquid ($x > 2$). The most concentrated sample (300 mg mL^{-1}), fitting to the SGR model at $x = 1.15$ would therefore be closer to the glassy state.

Strain-induced yielding is another rheological feature fitting to SGR. It has been predicted by Fielding *et al.*[39] in the framework of SGR model but it has never been verified experimentally to our knowledge. For $1 < x < 2$ the model predicts the onset of fluidization at a time $(t - t_W) \sim \left(\frac{1}{\sigma}\right)^{1/x-1}$, where $(t - t_W)$ corresponds to the elapsed time from the application of the stress. Actually we observe that concentrated collagen solutions fluidize at a deformation of about 50% (irrespective of the applied stress) and after an elapsed time t_C scaling as $\sigma^{-1/\alpha}$ with $\alpha \approx 0.3$, thus fitting to the SGR model at $x = 1.3$.

Long transients evidenced in recovery data also fit to SGR. As the creep period was the same for each run, the higher the stress amplitude, the more "fluidized" (or "hot" in SGR) the sample was at the end of the creep run. For instance, at the end of the creep test at $\sigma = 20$ Pa, $J(t)$ had not reached the regime where $J(t) \sim t$. The sample was not yet fluidized and could be considered at an "effective temperature" $1.3 < x < 2$ when recovery

started. Conversely, at $\sigma = 150$ Pa, the sample behaved like a fluid at the end of the creep run. It was at an "effective temperature" $x = 2$ when recovery started. Recovery from $\sigma = 20$ Pa was actually longer than recovery from $\sigma = 150$ Pa. This slowdown of the relaxation for x close to 1 is consistent with SGR model as a precursor to the onset of ageing for $x < 1$.

Eventually, the original "time–stress superposition principle" (TSS) here proposed is akin to the well-known "time–temperature superposition principle" (TTS) widely applied to polymer solutions or melts.[14] The stress dependence of the shift factor a_σ in TSS differs from the temperature dependence of the shift factor a_T in TTS. Nevertheless, this analogy suggests a similar role between mechanical and thermal energies in accelerating relaxation processes. This is in agreement with the SGR assumption of mechanically activated relaxation processes. Here, the spectrum of characteristic times scale as $\sigma^{-1/x-1}$ in both linear and non-linear regimes. Indeed, although the rescaling procedure is built exclusively on characteristics of the linear regime (power law exponent α, rescaling parameter $a_\sigma = \left(\frac{\sigma_0}{\sigma}\right)^{1/\alpha}$), it applies for the whole time range, including the long time non linear regime. In other words, with such a rescaling, even the non-linear part of the curves actually collapse onto the master curve, thereby justifying the applicability of TSS to the non linear regime in the time domain.

Although our experimental data fit rather well to the SGR model, the microscopic origin of the power-law viscoelasticity in collagen solutions remains to be elucidated. Indeed, SGR model is based on a mesoscopic description and ignore microscopic details. In particular, the nature of putative mesoscopic elements, the mechanism of their mutual rearrangements and the relationship with dominantly repulsive interactions are yet to be understood.

Anyway, TSS provides a powerful tool to extend the time domain accessible to rheometry, here up to seven orders of magnitude in time. This enables to predict when the sample will fluidize at any applied stress, provided that strain-induced yielding is observed for one particular stress amplitude. It would therefore be interesting to test whether TSS evidenced here for concentrated solutions of collagen could apply to other systems and to other values of α.

Links with fibrillogenesis and outlooks

Fibrillogenesis is the process by which collagen triple helices assemble laterally into ordered fibrils. Native fibrils found in biological tissues and formed *in vitro* have characteristic structural features, notably a regular stagger between adjacent triple helices resulting in a 67 nm period along the fibrils' main axis. Fibrillogenesis can be induced by increasing the pH of acidic solutions of collagen. At concentrations beyond about 5 mg mL^{-1}, neutral fibrillar gels are thereby obtained, where fibrils probably act as reticulation nodes.[40] As shown in Fig. 9, our previous data[5,41] combined to the abundant literature on precipitation from much more dilute solutions[9,42–44] indicate that the fibrils diameter d varies non-monotonously with the collagen concentration of the initial acidic solutions. Four concentration ranges can be distinguished in relation with changes in fibril size. Compared to our results, these domains (I–IV) roughly match

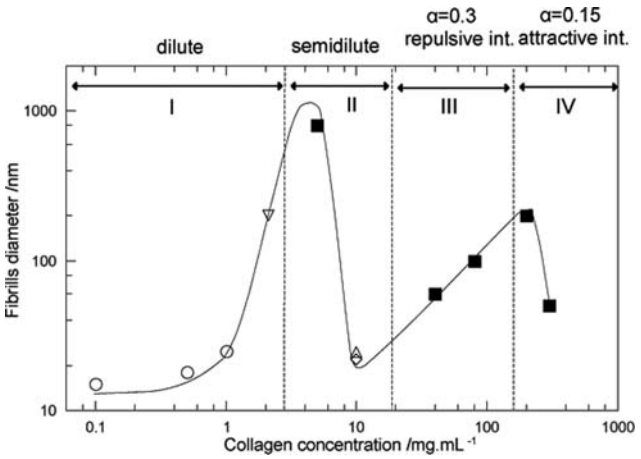

Fig. 9 Evolution of fibrils diameter as a function of collagen concentration. Fibrils diameters were determined in neutral conditions. Open symbols correspond to data taken from the literature, mostly from dilute solutions: ○ (open circles);[42] ▽ (open inverted triangle),[9] ◇ (open diamonds),[44] △ (open triangle).[43] Measurements at 5 mg mL^{-1}[41] and beyond 10 mg mL^{-5} are our data. Four domains can be distinguished: (i) domain I (1 μg mL^{-1}–5 mg mL^{-1}) and domain III (10–200 mg mL^{-1}) where d increases. (ii) Domain II (5–10 mg mL^{-1}) and domain IV (200–300 mg mL^{-1}) where d sharply decreases. These domains roughly match the distinct ranges identified combining rheometry and SAXS in acidic solutions of collagen: dilute, semidilute and power-law regimes with $\alpha = 0.3$ and $\alpha = 0.15$.

the concentration zones corresponding to different viscoelastic behaviours of the acidic solutions: domain I/dilute regime, domain II/semi-dilute regime, domain III/power-law regime with an exponent $\alpha = 0.3$ and dominant repulsive interactions between triple helices, domain IV/power-law regime with an exponent $\alpha = 0.15$ and dominant attractive interactions. This observation could be understood as follows: one can expect a higher topological connectivity between collagen molecules in domains II (steric overlap) and IV (attractive interactions), than in domains I (low volume fraction) and III (repulsive interactions competing with overlaps). One can further speculate that overlapping segments between collagen molecules in domains II and IV become nucleation points at the early stages of fibrillogenesis. However, the growth of the corresponding nuclei could be rapidly hindered, similarly to what is observed in polymer crystallization. Indeed, the ability of different portions of a single polymer molecule to participate in different nuclei is associated with entropic frustration and leads to incomplete crystallization.[45] This would favour the formation of numerous but small fibrils. In contrast, fewer nucleation points in domains I and III would lead to larger fibrils. Our results may thus suggest that the topological connectivity of the initial collagen solutions is a key parameter to control the fibril diameter in neutral gels. To that respect, shearing collagen solutions during fibrillogenesis may have significant effect on the self-assembly of collagen molecules and could thus be used as a control parameter in tissue engineering. Whether these results are relevant for *in vivo* fibrillogenesis remains an open question. The collagen precursor protein (procollagen) is secreted by cells in the extracellular space, where the enzymatic removal of the propeptides induces collagen

precipitation into fibrils.[46,47] Besides the specific role of collagens other than type I and of non-collagenous macromolecules known to participate in fibril diameter regulation,[43,48–51] molecular crowding in the cells vicinity may also influence fibrillogenesis. Considering the high collagen volume fractions determined in major connective tissues,[52,53] viscoelastic effects may therefore affect fibril formation *in vivo*.

Moreover, the viscoelastic properties of concentrated solutions of collagen are strikingly close to those of living cells. Indeed, power law viscoelastic behaviour has been reported for a wide variety of living cells with an exponent α ranging between 0.1 to 0.3, and prefactors of a few hundred Pa.[34–36] The SGR hypothesis has been put forward to explain cell mechanics providing a unifying explanation to the ability of the cytoskeletal lattice to deform, to flow and remodel.[54] It is rather intriguing that both the secreted collagen and the secreting cells have not only viscoleastic moduli of comparable magnitude, but also share the same weak power-law dependence on frequency.

Conclusion

In this study, we found that acidic solutions of collagen exhibited power-law viscoelastic spectra and strain-induced yielding at high concentration. These properties are consistent with "soft glassy rheology". The power exponent suggests fitting to the SGR model at $x = 1.3$, close to the soft glassy transition.

We showed that strain-induced yielding in creep experiments was described by a master curve resulting from a new time–stress superposition principle (TSS). From a fundamental point of view, it would be interesting to test whether TSS here evidenced for collagen solutions and for one particular value of α could be generic and apply to other values of α and other systems. TSS would then provide a powerful tool to predict the onset of the fluidization of such systems and their behaviour in time/stress domains that are not experimentally accessible. Eventually, we observed that the concentration domains corresponding to different rheological behaviours of the acidic solutions match the non monotonous evolution of fibrils diameter in neutral gels. This is of particular interest for the design of collagen-based functional materials for tissue engineering where controlling (or tuning) fibrils size in reconstituted collagen matrices is of major importance.

Appendix

Here we present the time–stress superposition principle applied to our creep data. The idea is to shift the creep curves $J(t,\sigma)$ along the logarithmic time and compliance axis by amounts required to bring them into superposition, then defining a master curve. In other words, the reduced compliance J_R is not a function of two variables (t,σ) but only of a combination of both: $J_R\left(\frac{t}{a_\sigma}\right)$ where a_σ is the stress-dependent time shift factor. Practically, the data are shifted in time to a reference curve $J_R\left(\frac{t}{a_\sigma(\sigma_0)}\right)$ corresponding to a reference stress σ_0 for which one has by definition $a_\sigma(\sigma_0) = 1$. The choice of σ_0 is of course arbitrary and a matter of convenience.

Since the dimension of the compliance $J(t,\sigma)$ is the inverse of a stress, the reduced compliance can be defined like:

$$J_R(t,\sigma) = \frac{J(t,\sigma)}{\left(\frac{1}{\sigma}\right)} = \sigma J(t,\sigma) \quad (1)$$

where σ is the applied stress. Therefore, $J_R(t,\sigma)$ corresponds to the strain $\gamma(t,\sigma)$ (the ratio between the shear displacement and the thickness of the sample).

The short-time regime, $J(t,\sigma) = At^\alpha$, can be rewritten in terms of reduced compliance as:

$$J_R(t,\sigma) = \gamma(t,\sigma) = \sigma A t^\alpha = A a_\sigma^\alpha \sigma \left(\frac{t}{a_\sigma}\right)^\alpha \quad (2)$$

To have J_R depending only on $\frac{t}{a_\sigma}$, the dimensionless quantity $(Aa_\sigma^\alpha\sigma)$ must be a constant that we name C.

It follows from $Aa_\sigma^\alpha\sigma = C$ that the shift factor a_σ can then be written as :

$$a_\sigma = \left(\frac{C}{A\sigma}\right)^{1/\alpha} \quad (3)$$

More accurately, since a_σ is equal to 1 for $\sigma = \sigma_0$, the constant C is equal to $A\sigma_0$ and then, eqn (2) and eqn (3) become:

$$\gamma(t,\sigma) = A\sigma_0 \cdot \left(\frac{t}{a_\sigma}\right)^\alpha \quad (4)$$

$$a_\sigma = \left(\frac{\sigma_0}{\sigma}\right)^{1/\alpha} \quad (5)$$

We arbitrarily chose $\sigma_0 = 20$ Pa to calculate the values of a_σ for each applied stress in the creep experiments reported on Fig. 5. In Fig. 7, the strains are reported as a function of the normalized time: $\gamma\left(\frac{t}{a_\sigma}\right)$ for each applied stress. All the curves indeed collapse onto a master curve, demonstrating that a time-stress superposition indeed applies to our data.

Acknowledgements

The authors thank H. Hamas for preliminary experiments, A. Asnacios, O. Cardoso and S. Lerouge for fruitful discussions.

References

1 J. Woodhead-Galloway. Collagen: the anatomy of a protein, In *Studies in Biology*, 1980, 117, London, Edward Arnold.
2 P. Fratzl, *Collagen Structure and Mechanics*, 2008, Springer-Verlag, New York.
3 L. Besseau and M.-M. Giraud-Guille, *J. Mol. Biol.*, 1995, **251**, 197–202.
4 G. Mosser, A. Anglo, C. Helary, Y. Bouligand and M.-M. Giraud-Guille, *Matrix Biol.*, 2006, **25**, 3–13.
5 F. Gobeaux, G. Mosser, P. Davidson, A. Anglo, P. Panine, M.-M. Giraud-Guille and E. Belamie, *J. Mol. Biol.*, 2008, **376**, 1509–1522.
6 J. Gross and D. Kirk, *J. Biol. Chem.*, 1958, **233**, 355–360.
7 G. C. Wood and M. K. Keech, *Biochem. J.*, 1960, **75**, 588–596.
8 G. C. Wood, *Biochem. J.*, 1960, **75**, 598–605.
9 Y. Li, A. Asadi, M. R. Monroe and E. P. Douglas, *Mater. Sci. Eng., C*, 2009, **29**, 1643–1649.

10 K. Claire and R. Pecora, *J. Phys. Chem. B*, 1997, **101**, 746–753.
11 T. Saito, N. Iso, H. Mizuno, N. Onda, H. Yamato and H. Odashima, *Biopolymers*, 1982, **21**, 715–728.
12 F. Henry, M. Nestler, S. Hvidt, J. D. Ferry and A. Veis, *Biopolymers*, 1983, **22**, 1747–1758.
13 H. Hofmann, T. Voss, K. Kühn and Engel, *J. Mol. Biol.*, 1984, **172**, 325–343.
14 J. D. Ferry, *Viscoelastic Properties of Polymers*, Wiley, New York, 1980.
15 A. C. Maggs, *Phys. Rev. E: Stat. Phys., Plasmas, Fluids, Relat. Interdiscip. Top.*, 1997, **55**, 7396–7400.
16 D. C. Morse, *Macromolecules*, 1998, **31**, 7044–7067.
17 G. Lai, Y. Li and G. Li, *Int. J. Biol. Macromol.*, 2008, **42**, 285–291.
18 G. Forgacs, S. A. Newman, B. Hinner, C. W. Maier and E. Sackmann, *Biophys. J.*, 2003, **84**, 1272–1280.
19 M. Djabourov, J.-P. Lechaire and F. Gaill, *Biorheology*, 1993, **30**, 191–205.
20 S. Hsu, A. M. Jamieson and J. Blackwell, *Biorheology*, 1994, **31**, 21–36.
21 D. M. Knapp, V. H. Barocas, A. G. Moon, K. Yoo, L. R. Petzold and R. T. Tranquillo, *J. Rheol.*, 1997, **41**, 971–993.
22 F. Gobeaux, E. Belamie, G. Mosser, P. Davidson, P. Panine and M.-M. Giraud-Guille, *Langmuir*, 2007, **23**, 6411–6417.
23 H. H. Winter and F. Chambon, *J. Rheol.*, 1986, **30**, 367.
24 M. Balland, N. Desprat, D. Icard, S. Féréol, A. Asnacios, J. Browaeys, S. Hénon and F. Gallet, *Phys. Rev. E: Stat., Nonlinear, Soft Matter Phys.*, 2006, **74**, 021911.
25 P. Sollich, F. Lequeux, P. Hébraud and M. E. Cates, *Phys. Rev. Lett.*, 1997, **78**, 2020–2024.
26 I. Bergman and R. Loxley, *Anal. Chem.*, 1963, **35**, 1961–1965.
27 W. W. Graessley, *Adv. Polym. Sci.*, 1974, **16**, 1.
28 T. Nishihara and P. Doty, *Proc. Natl. Acad. Sci. U. S. A.*, 1958, **44**, 411–417.
29 R. G. Larson. *The structure and rheology of complex fluids*, Oxford, Univ. Press, 1999.
30 L. C. A. Groot, M. E. Kuil, J. C. Leyte, J. R. C. Van der Maarel, R. K. Heenan, S. M. King and G. Jannick, *Liq. Cryst.*, 1994, **17**, 263–276.
31 E. E. Maier, R. Krause, M. Deggelmann, M. Hagenbüchle, R. Weber and S. Fraden, *Macromolecules*, 1992, **25**, 1125–1133.
32 K. R. Purdy, Z. Dogic, S. Fraden, A. Kühn, L. Lurio and S. G. J. Mochrie, *Phys. Rev. E: Stat., Nonlinear, Soft Matter Phys.*, 2003, **67**, 31708.
33 E. Belamie, P. Davidson and M.-M. Giraud-Guille, *J. Phys. Chem. B*, 2004, **108**, 14991–15000.
34 N. Desprat, A. Richert, J. Simeon and A. Asnacios, *Biophys. J.*, 2005, **88**, 2224–2233.
35 B. Fabry, G. N. Maksym, J. P. Butler, M. Glogauer, D. Navajas and J. J. Fredberg, *Phys. Rev. Lett.*, 2001, **87**, 148102–4.
36 J. Alcaraz, L. Buscemi, M. Grabulosa, X. Trepat, B. Fabry, R. Farre and D. Navajas, *Biophys. J.*, 2003, **84**, 2071–2079.
37 B. Suki, A. L. Barabasi and K. R. Lutchen, *J. Appl. Physiol.*, 1994, **76**, 2749–2759.
38 Y. Tseng and D. Wirtz, *Biophys. J.*, 2001, **81**, 1643–1656.
39 M. S. Fielding, P. Sollich and M. E. Cates, *J. Rheol.*, 2000, **44**(2), 323–369.
40 E. A. Sander, V. H. Barocas in , *Collagen Structure and Mechanics*, ed. Fratzl P, New York, USA, Springer, 2008, 475–504.
41 F. Gobeaux, PhD thesis, Université Pierre et Marie Curie, Paris, France, 2007.
42 R. L. Trelstad, K. Hayashi and J. Gross, *Proc. Natl. Acad. Sci. U. S. A.*, 1976, **73**(11), 4027–31.
43 G. D. Pins, D. L. Christiansen, R. Patel and F. H. Silver, *Biophys. J.*, 1997, **73**(4), 2164–2172.
44 D. L. Christiansen, E. K. Huang and F. H. Silver, *Matrix Biol.*, 2000, **19**(5), 409–420.
45 P. Welch and M. Muthukumar, *Phys. Rev. Lett.*, 2001, **87**(21), 218302.
46 R. L. Trelstad, Collagen fibrillogenesis *in vitro* and *in vivo*: the existence of unique aggregates and the special state of the fibril end, in *Extracellular Matrix Influences on Gene Expression*, ed. H. C. Slavkin and R. C. Greulich, 1975, pp. 331–339, Academic Press Inc., San Francisco, CA.
47 E. G. Canty and K. E. Kadler, *J. Cell Sci.*, 2005, **118**, 1341–1353.
48 A. D. Parry, M. H. Flint, G. C. Gillard and A. S. Craig, *FEBS Lett.*, 1982, **149**, 1–7.
49 D. E. Birk, J. M. Fitch, J. P. Babiarz, K. J. Doane and T. F. Linsenmayer, *J. Cell. Sci.*, 1990, **95**, 649–657.
50 D. E. Birk, *Micron*, 2001, **32**, 223–237.
51 U. Hansen and P. Bruckner, *J. Biol. Chem.*, 2003, **278**, 37352–37359.
52 Kjaer, H. Langberg, B. F. Miller, R. Boushel, R. Crameri, S. Koskinen, K. Heinemeir, J. L. Olesen, S. Døssing, M. Hansen, S. G. Pedersen, M. J. Rennie and P. Magnusson, *J. Musculoskelet. Neuronal. Interact.*, 2005, **5**, 42–52.
53 D. Taşkiran, E. Taşkiran, H. Yercan and F. Z. Kutay, *Tr. J. of Medical Sciences*, 1999, **29**, 7–9.
54 X. Trepat, G. Lenormand and J. J. Fredberg, Universality in cell mechanics, *Soft Matter*, 2008, **4**, 1750–1759.